Biodistribution, Dosimetry and Metabolism of 11β-Methoxy-(17α,20E/Z)-[^{123}I]Iodovinylestradiol in Healthy Women and Breast Cancer Patients

Oussama Nachar, Jacques A. Rousseau, Bernard Lefebvre, René Ouellet, Hasrat Ali and Johan E. van Lier

Department of Nuclear Medicine and Radiobiology, Faculty of Medicine, Université de Sherbrooke, Sherbrooke, Québec, Canada

The biodistribution and dosimetry of the 20E and 20Z stereoisomers of 11β-methoxy-(17α,20)-[^{123}I]iodovinylestradiol (MIVE) were evaluated in six healthy women. Tumor uptake and metabolism of the 20Z isomer were evaluated in 13 women referred after abnormal mammography or after discovery of a suspect mass at physical examination. **Methods:** The radiopharmaceuticals were prepared from their corresponding stannyl intermediates and administrated intravenously. Blood samples were drawn at different time intervals and urine was collected for up to 24 h. Metabolites were detected by radiochromatography. Tissue distribution was followed for up to 24 h by scintigraphic imaging. The dosimetry was computed according to the Medical Internal Radiation Dose scheme. **Results:** The 20E and 20Z isomers exhibit similar biodistribution and dosimetry patterns. Chromatographic analysis of plasma samples of healthy volunteers and cancer patients, as well as in vitro plasma incubations, confirmed the in vivo stability of (20Z)-[^{123}I]MIVE. Radioactivity was rapidly cleared from the blood by the liver and excreted through the gut, which received the highest radiation dose (0.211 mGy/MBq). The effective doses for the adult female and male phantom were 0.054 and 0.046 mSv/MBq, respectively. Among the 13 patients imaged with (20Z)-[^{123}I]MIVE, 3 had fibrocystic disease with no focal uptake, 8 had good agreement with in vitro estrogen receptor determination and 2 were false-positive. **Conclusion:** The radiation dose after intravenous administration of 20E- or (20Z)-[^{123}I]MIVE at imaging dose levels is within acceptable limits. There was a good correlation between uptake of (20Z)-[^{123}I]MIVE and the presence of estrogen receptors in breast cancer patients.

Key Words: estrogen receptors; iodovinylestradiol; 11β-methoxy-(17α,20E/Z)-[^{123}I]iodovinylestradiol; ^{123}I; breast cancer; SPECT

J Nucl Med 1999; 40:1728–1736

Knowledge of the status of estrogen receptors (ERs) is an important factor for the proper management of breast cancer patients (*1–3*). About two thirds of breast cancer patients are ER positive, and, at present, such ER levels are measured in vitro after resection of the tumor (*4*). This technique, however, is susceptible to error because of the heterogeneity of ER distribution within the tumor (*5*) and does not provide information on the presence of ER in metastases or on changes that may occur in functionality during the course of treatment (*6,7*). An alternative to the biopsy procedure is scintimammography (SMM) using radiolabeled estrogens with a high affinity and specificity for ER (*8*). Among the radiopharmaceuticals that have been advanced for this purpose, ^{18}F-labeled 16α-fluoroestradiol (FES) gave reliable images of both primary and metastatic breast cancer (*9–11*). However, because of its short half-life ($t_{½}$) of 110 min, production of the positron-emitting ^{18}F isotope requires an in-house cyclotron facility. Other radioisotopes that have been used successfully to label estrogens for in vivo imaging of ER include various isotopes of iodine. Only the ^{123}I-labeled derivatives have been used in a clinical setting, and preliminary reports on ER imaging of human breast cancer have appeared. The site of attachment of radioiodine onto the estradiol skeleton is restricted to two positions, i.e., the 16α-position of 17β-estradiol and the 20E/Z positions of 17α-iodovinylestradiol (IVE). Substitution at most other positions results in loss of target selectivity. Although a few studies with 16α-[^{123}I]iodoestradiol have been reported, rapid metabolism limits the clinical usefulness of this agent (*8,12–14*). In contrast, 17α-iodovinylestradiol derivatives exhibit good in vivo stability. The iodovinyl derivatives can be obtained in either the 20Z (trans) or 20E (cis) configuration. Earlier studies on the in vitro and in vivo properties of the IVE concerned the thermodynamically more stable 20E isomer (*15,16*), and the first clinical assays were likewise conducted with this isomer (*17*). In 1988 our laboratory reported the synthesis of both (20E)- and (20Z)-[^{125}I]IVE, and we showed that the 20Z isomer exhibits higher ER-binding affinity and better in vivo ER-mediated target tissue uptake compared with the 20E isomer (*18*). Additional substitutions on the IVE at either the 11β-, 7α- or 4-position (or all three) subsequently led to the development of analogs with good affinity for the ER, increased metabolic stability and decreased nonspecific binding affinities for plasma proteins resulting in substantial higher target selectivity (*19*). Among these derivatives, the highest in vivo ER-mediated target tissue uptake in laboratory animals was observed with (20Z)-MIVE, the 11β-methoxy derivative of

Received Nov. 12, 1998; revision accepted Mar. 10, 1999.

For correspondence or reprints contact: Johan E. van Lier, PhD, Department of Nuclear Medicine and Radiobiology, Faculty of Medicine, Université de Sherbrooke, 3001, 12th Ave. N., Sherbrooke, Québec, Canada J1H 5N4.

(20Z)-IVE (Fig. 1) (*20,21*). However, the in vivo stability of the 20Z isomer has been questioned because interconversion to the 20E isomer has been reported to occur in the rat (*22*).

The potential of ^{123}I-radiolabeled MIVE for breast tumor ER imaging was investigated in two independent clinical trials. Earlier studies with the 20E isomer in 19 patients with primary and metastatic breast cancer showed a poor correlation between the presence of ER and tumor uptake (*17*). Results from a second clinical trial in 25 patients with (20Z)-[^{123}I]MIVE revealed that 90% of the primary tumors and 80% of the metastatic lesions could be delineated (*23*). In this study we compare the biodistribution and excretion of the 20E and 20Z isomers of [^{123}I]MIVE in human subjects. The dosimetric values for both the standard male and female phantoms are presented. The results of scintigraphic imaging with (20Z)-[^{123}I]MIVE in 10 patients referred after suspect mammography are reported along with a correlation between tumor uptake and in vitro ER quantification. The in vivo stability of the 20Z isomer of [^{123}I]MIVE is also addressed.

MATERIALS AND METHODS

Materials

All chemicals used were commercially available and of the highest chemical grade available. The carrier-free ^{123}I-iodide ($t_{½}$ = 13.2 h, γ = 159 keV) was obtained as a weak NaOH solution from MDS Nordion (Kanata, Ontario, Canada). The 20% Intralipid (Pharmacia, Mississauga, Ontario, Canada) and ethanol used for the parenteral administration of the radiopharmaceuticals were obtained from the hospital pharmacy and were certified sterile and pyrogen free. Analytical thin-layer chromatography (TLC) was performed on silica gel plates PE SIL-G/UV$_{254}$ (Whatman, Maidstone, UK) eluted with a mixture of chloroform and acetonitrile (10:1), and radioactivity was visualized with a Packard Instantimager (Packard, Meriden, CT). High-performance liquid chromatography (HPLC) was performed on a Varian 5000 instrument (Varian Corp., Walnut Creek, CA) on a reversed-phase column (C_{18}, ODS-2 column, 4 µm, 10 × 1 cm; Waters, Milford, MA) eluted with a mixture of methanol and water (70:30). Products were detected at λ = 280 nm and, where appropriate, by their γ radiation, which was registered via a sodium iodine detector. Dose activities were measured in an Accucal 2001 dose calibrator (Nuclear Pharmacy Inc., Albuquerque, NM). The radioactivity of blood and urine samples was measured in an LKB model 1282 Compugamma gamma counter (Wallac, Turku, Finland). Whole-body images were recorded with a Starcam 4000i XRT gamma camera (General Electric, Saint Albans, UK) equipped with a parallel, low-energy, high-resolution collimator. Image analysis was performed on a Genie PNR model nuclear medicine-dedicated computer (General Electric). Pyrogenicity was measured by the *Limulus* amoebocyte lysate method according to the recommendation of the manufacturer (Biowhittaker Inc., Walkersville, MD). In vitro quantification of ERs and progesterone receptors (PRs) in breast tumor biopsies was achieved with the Abbott ER-EIA and PgR-EIA monoclonal kits (Abbott Laboratories, Abbott Park, IL).

Synthesis

The 20E and 20Z isomers of MIVE were prepared from their corresponding 20E and 20Z isomers of 11β-methoxy-(17α,20)-21-tributylstanylestradiol as described (*20,24,25*). The 20E/Z-tributylstannyl isomers were freshly purified by reversed-phase HPLC (Waters C_{18}, ODS-2 column, 4 µm, 1 × 10 cm) using a gradient of methanol and water (95:5) to methanol (100%) over 20 min at a flow rate of 1 mL/min. Eluting steroids were detected at 280 nm, and the stannyl product was collected (t_R = 30 min). After evaporation of the solvent, the 20E- or 20Z-stannyl derivative (40 µg, 0.064 µmol) was dissolved in 120 µL ethanol. To this was added the no-carrier-added (NCA) ^{123}I solution, consisting of 20 µL AcOH (pH 3–4) and [^{123}I]iodine in 244 µL diluted NaOH (481 MBq). To the mixture was added 50 µL (0.37 µmol) of N-chlorosuccinimide in methanol (1 mg/mL). After vigorous agitation for 5 min at 25°C, 20 µL (0.4 µmol) of a 10 mg/mL solution of sodium thiosulfate were added. The reaction mixture was purified by HPLC in five 100-µL batches using a reversed-phase column eluting with a mixture of methanol and water (70:30) at 1 mL/min. The unreacted radioiodine eluted at 3–4 min, [^{123}I]MIVE eluted at 12–14 min and the stannyl starting material eluted at 35 min. After complete evaporation of the collected fraction under nitrogen, [^{123}I]MIVE was transferred to a sterile hood, dissolved in two times 1.0 mL ethanol, transferred into a sterile and pyrogen-free vial through a dry 0.22-µm filter and evaporated to dryness under air (filtered over a 0.22-µm filter) while heating gently with a hair dryer.

Formulation

To the vials containing the dry [^{123}I]MIVE were added 0.2–0.4 mL ethanol and 2–4 mL 20% Intralipid. The Intralipid was added rapidly to the ethanol while swirling the vial. An aliquot of the preparation was retained for pyrogenicity testing. The content of the vial was transferred to a syringe, and the activity was measured in a dose calibrator. A sample from each preparation was stored at −20°C for sterility testing in the event that a patient presented adverse effects.

Patients and Healthy Volunteers

An internal review board approved the clinical protocol, and all participants gave informed consent. Six healthy women (age 20–30

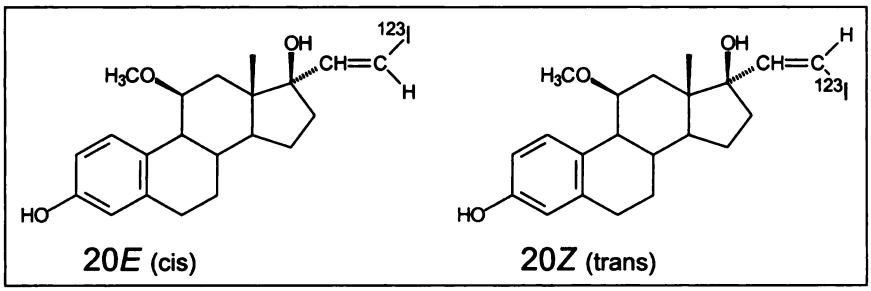

FIGURE 1. Structures of 20E and 20Z isomers of [^{123}I]MIVE.

y, mean weight 59.5 ± 10.8 kg) were recruited for the dosimetry and biodistribution study. Medical examination and questionnaire responses indicated that they were healthy. Breast imaging was also performed in 13 patients referred after an abnormal mammography or a suspect mass at physical examination. A negative pregnancy test was required from all women of childbearing age before enrollment in the study. Each subject was given 150 mg saturated potassium iodine (SSKI) solution orally the day before the examination and again 1 h before the administration of the tracer. With the healthy volunteers, we compared the 20E and 20Z preparations at the same time after onset of menstruation. For cancer patients, we were bound by the specific treatment protocol.

Imaging

From 1 to 2 mL (5–75 MBq) [^{123}I]MIVE were administrated intravenously while each woman rested on the imaging table. The injection site was imaged in the minutes after administration to ensure that there was no tissue infiltration. For all acquisitions, the windows of the camera were open at 20% and adjusted on the 159-keV photoelectric peak of ^{123}I. For biodistribution and dosimetry, each subject received both the 20E and the 20Z isomers of [^{123}I]MIVE administrated at intervals of about 1 mo. Whole-body scanning was done at a rate of 10 cm/min, keeping the camera-to-patient distance constant. Anterior and posterior whole-body imaging was performed at 1, 3, 6, 9 and 24 h after injection. Breast cancer patients received only (20Z)-[^{123}I]MIVE. Scintigraphic imaging of the breast and of the axillary region was performed immediately and at 1 and 3–24 h after administration of the radiopharmaceutical.

For biodistribution and dosimetry calculations, the time-activity curves for the whole body, brain, lungs, liver, gallbladder and abdomen were obtained from the scintigraphic images by tracing regions of interest (ROIs) around the selected organs. The geometric mean of the anterior and posterior view for each ROI was used to compute the percent injected dose (%ID) values. The geometric mean of the counts in the whole body scintigram at 1 h after injection was corrected for radioactive decay from the time of injection:

$$(\text{Activity}_{(\text{at injection time})} = \text{Activity}_{(\text{at 1 h})} \times \exp^{(\lambda \times 1\ \text{h})}), \quad \text{Eq. 1}$$

this value being taken as 100 %ID. For patients, two nuclear medicine specialists independently interpreted the images as positive (MIVE focal uptake) or negative (no focal uptake). Tumor-to-nontumor ratios were obtained by drawing ROIs around the tumor area and an area of similar size on the adjacent breast tissue. These results were then compared with the tumor ER concentration that was determined in vitro after surgery and tumor resection. A receptor concentration exceeding 9 fmol/mg protein was considered ER positive.

Blood Clearance in Healthy Volunteers

From 2 to 4 mL blood were drawn in a heparinized Vaccutainer tube (Becton Dikinson, Franklin Lakes, NJ) through a catheter that was installed in a vein contralateral to the injection site. Blood samples were collected at 5 min and at 1, 3, 6, 9 and 24 h after injection. The plasma was separated from the cellular material by centrifugation for 10 min at 10,000 rpm in an Eppendorf microcentrifuge (Brinkmann Instruments Co., Westbury, NY). The kinetic parameters of plasma clearance were computed from the %ID/g of plasma using PHKIT software (*26*) and the sum of two exponential term models.

Urinary Excretion in Healthy Volunteers

All urine samples were collected over the 24-h period after administration of the radiopharmaceutical. The weight and radioactivity of urine collected at each micturition were determined, and specific activity was calculated.

Counting of Samples

The specific activities of blood, plasma and urine were obtained by counting the collected samples of known weight along with a known volume of the injected preparation. The windows of the gamma counter were adjusted at the 159-keV photo peak of ^{123}I with a 20% window. All values were corrected for background.

Dosimetry in Healthy Volunteers

The residence times for the brain, thyroid, gallbladder, liver, lungs and the remainder of the body were computed by dividing the area under their %ID/h curves by the 100 %ID value. Before integration, the time-activity curves were fitted to a gamma function with an exponential tail ($r > 0.96$):

$$A(t \exp^{-Bt} + C(1 - \exp^{-Dt})\exp^{-Et}), \quad \text{Eq. 2}$$

assuming that tissue specific activity was zero at time zero (*27*).

The absorbed dose was computed from the residence time according to the Medical Internal Radiation Dose (MIRD) scheme using MIRDOSE 3.1 software (Oak Ridge National Laboratories, Oak Ridge, TN) (*28,29*). The adult female and male phantoms were selected. The residence time for the gastrointestinal tract was estimated from the fraction of the administrated activity found in the abdomen using the gastrointestinal module of the MIRDOSE program.

For the determination of bladder residence time, a model was designed to take into account the irregular voiding pattern observed among the volunteers. In this model the experimental data of the biological urinary clearance are used to generate a time-activity curve for each micturition. Each triangular area represents one micturition cycle (i) (Fig. 2). For each micturition, the volume of urine, V_i (mL), the amount of radioactivity voided, A_i (%ID), and the filling time of the bladder, $\Delta_i t = t_i - t_{i-1}$ (in hours), are known. Assuming that the filling rate is constant for a given micturition (i), the bladder filling rate, $\alpha_i = V_i/\Delta_i t$ (mL/h), and the specific activity of the urine, $As_i = A_i/V_i$ (%ID/mL), can be determined. Therefore, the amount of radioactivity found in the bladder for each cycle (i) at any given time between t_{i-1} and t_i is given in Equation 3, which takes into account the loss of radioactivity through disintegration:

$$A_i(t) = As_i\alpha_i(t - t_{i-1})\exp(-\lambda t). \quad \text{Eq. 3}$$

The residence time for the bladder is then obtained by summing the areas under the time-activity curve of each micturition (i) and dividing by the 100 %ID:

$$A = \sum_{i=1}^{n} \int_{t_{i-1}}^{t_i} As_i\alpha_i(t - t_{i-1})\exp(-\lambda t)\, dt, \quad \text{Eq. 4}$$

where n = the total number of micturitions and A = the total activity accumulated in the bladder over 24 h (MBq/h and λ = 0.0525 h^{-1} for ^{123}I.

Stability of (20Z)-[^{123}I]MIVE in Human Plasma

To establish the stability in plasma, the (20Z)-MIVE labeled with long-lived ^{125}I isotope was incubated in freshly drawn plasma from healthy women and female rats. Blood samples were collected in ethylenediaminetetraacetic acid- or heparin-coated Vaccu-

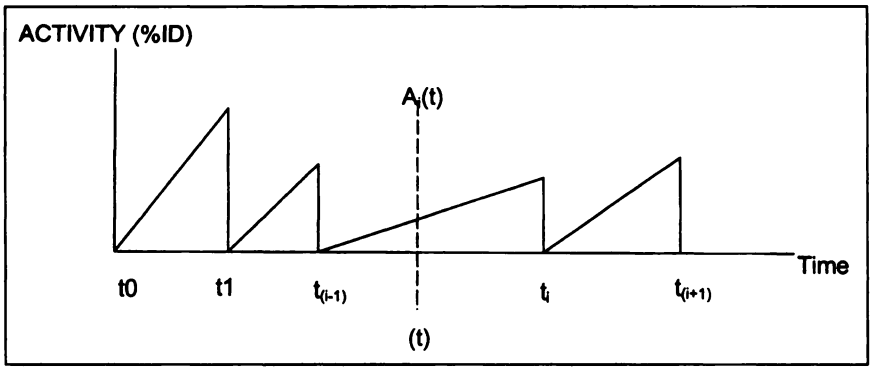

FIGURE 2. Mathematical modeling of irregular voiding pattern observed for bladder.

tainer tubes (Becton Dickinson). The plasma was isolated by centrifugation. The samples were incubated at 37°C in a water bath before the addition of radiolabeled MIVE as a 9% ethanol and saline and 1% Intralipid emulsion (0.1 mL/mL plasma). Incubation was continued for up to 6 h, and samples were vortexed every 30 min. All samples were extracted with ethyl acetate and analyzed by silica TLC along with unlabeled (20E)- and (20Z)-MIVE. The TLC plates were developed twice in a mixture of chloroform and acetonitrile (10:1); in this way (20Z)- and (20E)-MIVE are well separated, with R_f values of 0.39 and 0.28, respectively. The plates were scanned for radioactivity with an Instantimager; the unlabeled steroids were visualized by sulfuric acid spraying and heating. Plasma samples from healthy volunteers, cancer patients and rats injected with (20Z)-[^{123}I]MIVE were also analyzed as described.

Statistical Analysis

Values are given as mean ± SD. Noncontinuous variables were compared with the Fisher exact test.

RESULTS

The labeling yield of the 20E or 20Z isomers of [^{123}I]MIVE ranged from 50% to 80% with a radiochemical purity exceeding 95% as determined by HPLC. Pyrogeneity of the injected preparation was lower than 0.12 endotoxin unit per milliliter. No side effects were noticed after the parenteral administration of [^{123}I]MIVE. The effective biodistribution values are given in Table 1. The results are expressed as %ID in whole organ. SSKI proved to be effective in blocking thyroid uptake of free radioiodine because only marginal thyroid uptake was noticed in some subjects. Both isomers of MIVE share a similar biodistribution pattern. Blood clearance follows a two-exponential model. The first phase is over within minutes after injection, when the bulk of radioactivity is trapped by the liver, and the remaining blood radioactivity is cleared at rates of $t_{1/2}$ = 3 h and $t_{1/2}$ = 4 h for

TABLE 1
Effective Tissue Distribution of [^{123}I]MIVE

	20E isomer				
Site	1 h	3 h	6 h	9 h	24 h
Brain	1.12 ± 0.22	0.61 ± 0.15	0.42 ± 0.12	0.34 ± 0.15	0.23 ± 0.10
Thyroid	0.35 ± 0.07	0.23 ± 0.05	0.16 ± 0.02	0.12 ± 0.05	0.07 ± 0.02
Lungs	4.76 ± 0.64	2.96 ± 0.61	2.11 ± 0.54	1.59 ± 0.59	0.84 ± 0.27
Liver	6.81 ± 1.10	3.67 ± 1.00	2.73 ± 0.81	2.07 ± 0.78	0.82 ± 0.32
Gallbladder	2.14 ± 1.91	1.87 ± 1.52	0.75 ± 0.44	0.37 ± 0.20	0.14 ± 0.12
Abdomen	27.85 ± 8.13	28.72 ± 8.87	28.64 ± 5.98	22.19 ± 6.32	9.93 ± 2.06
Bladder	2.82 ± 1.25	1.81 ± 0.59	1.22 ± 0.27	1.22 ± 0.69	0.48 ± 0.34
Whole body	86.49 ± 6.64	70.43 ± 5.12	58.63 ± 5.24	45.11 ± 13.6	22.14 ± 6.88
	20Z isomer				
	1 h	3 h	6 h	9 h	24 h
Brain	1.07 ± 0.40	0.56 ± 0.18	0.36 ± 0.13	0.29 ± 0.09	0.17 ± 0.07
Thyroid	0.49 ± 0.07	0.44 ± 0.20	0.21 ± 0.02	0.17 ± 0.02	0.08 ± 0.02
Lungs	5.21 ± 0.56	3.12 ± 0.45	2.04 ± 0.29	1.64 ± 0.22	0.74 ± 0.18
Liver	6.74 ± 1.07	3.40 ± 0.78	2.32 ± 0.56	1.86 ± 0.69	0.75 ± 0.20
Gallbladder	3.32 ± 1.99	1.53 ± 1.16	0.72 ± 0.22	0.35 ± 0.11	0.14 ± 0.04
Abdomen	28.64 ± 4.79	30.34 ± 3.44	28.52 ± 0.92	25.02 ± 1.12	10.04 ± 0.54
Bladder	6.78 ± 4.02	2.39 ± 1.16	1.02 ± 0.38	0.77 ± 0.45	0.19 ± 0.13
Whole body	91.15 ± 5.12	71.46 ± 3.85	55.55 ± 1.59	46.31 ± 1.52	20.75 ± 3.06

MIVE = 11β-methoxy-(17α,20E/Z)-[^{123}I]iodovinylestradiol.
Data are expressed as percentage of injected dose per gram of tissue in healthy volunteers, ±SD.

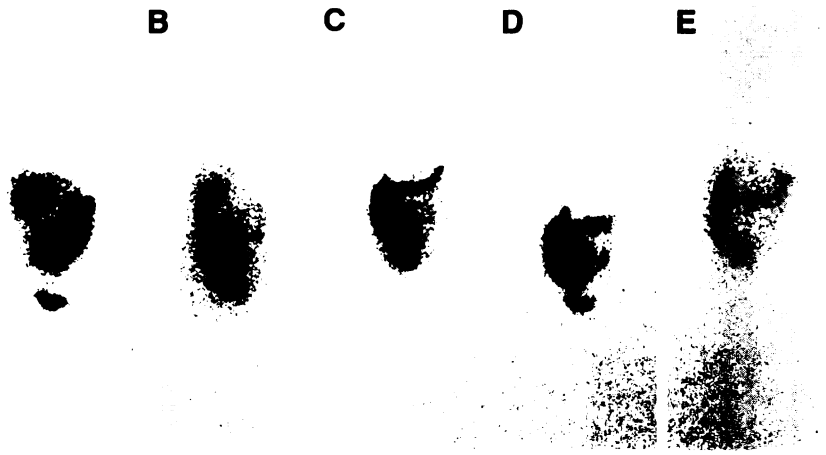

FIGURE 3. Anterior whole-body scintigraphic images of healthy woman after intravenous administration of 111 MBq (20Z)-[^{123}I]MIVE at 1 (A), 3 (B), 6 (C), 9 (D) and 24 (E) h.

the 20E and 20Z isomers, respectively. At 3 h after injection most radioactivity has passed from the gallbladder to the intestine (Fig. 3). The retention time in the liver is very short; once in the intestine the radioactivity is eliminated at the normal gastrointestinal excretion rate. In some subjects the presence of radioactivity in the breast was noted. As much as 45% (20Z isomer) and 31% (20E isomer) of the administrated radioactivity was excreted in the urine within 24 h after administration. The specific activity of the urine was highest immediately after injection and decreased thereafter. HPLC analysis revealed that roughly half of the radioactivity found in the urine was free iodine.

Stability of (20Z)-[^{123}I]MIVE in Human Plasma

It has been reported that after intraperitoneal administration to rats or incubation at 25°C in rat plasma, the 20Z isomer of [^{125}I]MIVE is rapidly converted to the 20E isomer, which is the more stable steric conformation (22). To establish whether this transformation also takes place in human plasma, we analyzed, by TLC, samples from volun-

TABLE 2
Residence Times (Hours in Healthy Volunteers)

	(20E)-MIVE						
Site	Subject 1	Subject 2	Subject 3	Subject 4	Subject 5	Subject 6	Average ± SD
Brain	0.096	0.105	0.052	0.143	0.080	0.092	0.09 ± 0.02
Gallbladder	0.090	0.074	0.040	0.211	0.229	0.105	0.12 ± 0.07
Lower large intestine	1.980	2.350	2.190	1.770	2.090	2.350	2.12 ± 0.22
Small intestine	1.260	1.490	1.390	1.120	1.320	1.490	1.34 ± 0.15
Upper large intestine	2.430	2.870	2.680	2.170	2.550	2.870	2.59 ± 0.27
Liver	0.636	0.487	0.270	0.689	0.506	0.636	0.54 ± 0.15
Lungs	0.452	0.386	0.280	0.616	0.360	0.399	0.42 ± 0.12
Thyroid	0.042	0.035	0.028	0.040	0.026	0.024	0.03 ± 0.01
Urinary bladder	0.420	0.700	1.320	0.400	0.420	0.760	0.67 ± 0.34
Remainder	7.58	3.970	2.610	7.890	3.570	3.630	4.87 ± 0.25
	(20Z)-MIVE						
	Subject 1	Subject 2	Subject 3	Subject 4	Subject 5	Subject 6	Average ± SD
Brain	0.054	0.110	0.073	0.107	0.062	*	0.08 ± 0.00
Gallbladder	0.163	0.210	0.079	0.217	0.103	*	0.15 ± 0.07
Lower large intestine	2.190	2.030	2.190	1.980	2.090	*	2.1 ± 0.09
Small intestine	1.390	1.290	1.390	1.260	1.320	*	1.33 ± 0.07
Upper large intestine	2.680	2.490	2.680	2.430	2.550	*	2.57 ± 0.11
Liver	0.334	0.545	0.383	0.597	0.563	*	0.48 ± 0.11
Lungs	0.401	0.403	0.494	0.454	0.377	*	0.43 ± 0.04
Thyroid	0.056	0.034	0.037	0.048	0.044	*	0.04 ± 0.01
Urinary bladder	0.640	0.990	0.340	0.820	0.620	*	0.68 ± 0.25
Remainder	4.94	4.010	3.650	4.450	3.380	*	4.09 ± 0.63

*The activity administrated was too low to give reliable residence time values.
MIVE = 11β-methoxy-(17α,20E/Z)-[^{123}I]iodovinylestradiol.

teers and cancer patients who had received the 20Z isomer of [^{123}I]MIVE. Because of the rapid disappearance of [^{123}I]MIVE from the blood pool, it was difficult to recover radiolabeled steroids and their products for analysis. In 3 persons, however, enough radioactivity was recovered to show that (20Z)-[^{123}I]MIVE remained unaltered for up to 1 h after injection. At 3 h after injection (1 person), the recovered radioactivity migrated at higher R_f values, indicating the formation of metabolites. In view of these results, we incubated the longer-lived (20Z)-[^{125}I]MIVE with human and rat plasma for up to 24 h. TLC analysis and autoradiography showed that (20Z)-[^{125}I]MIVE retained its configuration under these experimental conditions.

Dosimetry

The residence times for the 20E- and 20Z-MIVE are similar and comparable to the values published by Rijks et al. (*30*) for the 20Z isomer (Table 2). The longest residence times were observed for the gastrointestinal tract, the gallbladder and the urinary bladder. The radiation dose estimates were computed for each subject independently, and the average values are presented in Table 3. The data were processed for the adult standard man and women models. The organs that received most of the radiation burden were the lower and upper large intestines, i.e., 0.211 and 0.193 mGy/MBq, respectively. The reproductive organs received 0.03 mGy/MBq (uterus) and 0.05 mGy/MBq (ovaries) from abdominal radioactivity. The dosimetry values of (20E)- and (20Z)-[^{123}I]MIVE are similar. The 0.054 and 0.046 mSv/MBq effective doses calculated for the adult female and male phantoms are well within the acceptable dose and translate to a total radiation burden of 7 mSv per examination (150 MBq). For comparison, administration of ^{99m}Tc-MIBI, which is routinely used for scintimammography, results in a total dose of 5 mSv per examination (1000 MBq).

Scintimammography

Among the 13 patients (Table 4), 10 were subsequently diagnosed with breast cancer. The 3 cancer-free patients showed no focal uptake of (20Z)-[^{123}I]MIVE. The (20Z)-[^{123}I]MIVE uptake in cancer patients correlated well with in vitro ER determinations ($P = 0.08$) (Table 4, Fig. 4). For the patients showing (20Z)-[^{123}I]MIVE uptake, the average tumor-to-nontumor ratio was 2 ± 0.4.

DISCUSSION

In this study, we measured the whole-body biodistribution of a new ER-based ^{123}I-radiopharmaceutical, MIVE. The

TABLE 3
Radiation Dose Estimate After Intravenous Administration of 20E and 20Z Isomers of [^{123}I]-MIVE (mGy/MBq)

Organ	(20E)-[^{123}I]MIVE		(20Z)-[^{123}I]MIVE	
	Female phantom	Male phantom	Female phantom	Male phantom
Adrenals	0.010 ± 0.0038*	0.0081 ± 0.001	0.009 ± 0.0007	0.0061 ± 0.0011
Brain	0.004 ± 0.0016	0.0037 ± 0.0005	0.004 ± 0.0008	0.0027 ± 0.0005
Breast	0.004 ± 0.0026	0.0039 ± 0.0006	0.004 ± 0.0005	0.0030 ± 0.0005
Gallbladder wall	0.057 ± 0.0206	0.0485 ± 0.0074	0.064 ± 0.0163	0.0465 ± 0.0095
Lower large intestine wall	0.211 ± 0.0196	0.1892 ± 0.0075	0.209 ± 0.0083	0.1566 ± 0.0300
Small intestine	0.084 ± 0.0062	0.0684 ± 0.0022	0.083 ± 0.0032	0.056 ± 0.0108
Stomach	0.014 ± 0.003	0.0154 ± 0.0039	0.014 ± 0.0008	0.0096 ± 0.0012
Upper large intestine wall	0.193 ± 0.0170	0.1652 ± 0.0064	0.190 ± 0.0077	0.1366 ± 0.0261
Heart wall	0.008 ± 0.0039	0.0066 ± 0.001	0.008 ± 0.0007	0.005 ± 0.0008
Kidneys	0.011 ± 0.0031	0.0098 ± 0.0008	0.011 ± 0.0007	0.0076 ± 0.0014
Liver	0.021 ± 0.0052	0.0168 ± 0.0016	0.020 ± 0.0030	0.0131 ± 0.0025
Lungs	0.017 ± 0.0053	0.0137 ± 0.0016	0.018 ± 0.0015	0.0115 ± 0.0020
Muscle	0.010 ± 0.0026	0.0082 ± 0.0006	0.009 ± 0.0007	0.0064 ± 0.0012
Ovaries	0.050 ± 0.0027	0.0395 ± 0.001	0.050 ± 0.0017	0.0321 ± 0.0062
Pancreas	0.012 ± 0.0038	0.0101 ± 0.001	0.012 ± 0.0009	0.0075 ± 0.0013
Red marrow	0.011 ± 0.0024	0.0094 ± 0.0006	0.011 ± 0.0006	0.0074 ± 0.0014
Bone surface	0.014 ± 0.0051	0.0125 ± 0.0012	0.014 ± 0.0011	0.0096 ± 0.0017
Skin	0.005 ± 0.0021	0.0041 ± 0.0005	0.004 ± 0.0005	0.0031 ± 0.0005
Spleen	0.009 ± 0.0034	0.0077 ± 0.0008	0.009 ± 0.0007	0.0057 ± 0.001
Testes	—	0.0068 ± 0.0005	—	0.0052 ± 0.0010
Thymus	0.006 ± 0.0035	0.0049 ± 0.0008	0.006 ± 0.0007	0.0038 ± 0.0006
Thyroid	0.044 ± 0.0109	0.0369 ± 0.0038	0.058 ± 0.0110	0.0410 ± 0.0082
Urinary bladder wall	0.088 ± 0.0382	0.0614 ± 0.0104	0.089 ± 0.0265	0.0531 ± 0.0107
Uterus	0.030 ± 0.0027	—	0.030 ± 0.0018	—
Total body	0.012 ± 0.0026	0.0101 ± 0.0006	0.012 ± 0.0007	0.0079 ± 0.0015
Effective dose equivalent*	0.056 ± 0.0027	0.045 ± 0.0012	0.057 ± 0.0024	0.389 ± 0.0076
Effective dose*	0.054 ± 0.0030	0.046 ± 0.0015	0.054 ± 0.0017	0.0375 ± 0.0072

*Units of effective dose equivalent and effective dose are in mSv/MBq.
MIVE = 11β-methoxy-(17α,20E/Z)-[^{123}I]iodovinylestradiol.

TABLE 4
Comparison of Results of (20Z)-[^{123}I]MIVE Scintimammography and In Vitro Determination of Tumoral Estrogen Receptor Concentrations

Subject no.	Age (y)	Status	Node	Grade*	Size (cm)	ER/PR†	MIVE‡
7	55	Lobular carcinoma of left breast	—	—	2.0	Neg/Neg	Pos
8	43	Fibrocystic disease	—	—	—	—	Neg
9	54	Invasive ductal carcinoma of left breast. Poorly differentiated	0/17	III/III	2.0	Neg/Neg	Neg
10	42	Infiltrating ductal carcinoma of left breast	1/18	II/III	2.0	Neg/38	Neg
11	40	Fibrocystic disease	—	—	—	—	Neg
12	56	Ductal carcinoma of left breast. Moderately differentiated	0/9	II/III	—	81/30	Pos
13	45	Fibrocystic disease	—	—	—	—	Neg
14	69	Infiltrating ductal carcinoma of left breast	1/12	II/III	2.5	Neg/Neg	Neg
15	73	Infiltrating ductal carcinoma of left breast	0/0	II/III	2.5	Neg/Neg	Neg
16	79	Invasive ductal carcinoma of left breast	0/0	III/III	2	60/95	Pos
17	55	Infiltrating lobular carcinoma of right breast	0/0	—	13.0	Neg/16	Pos
18	55	Infiltrating ductal carcinoma of right breast	0/0	III/III	4.0	Neg/Neg	Neg
19	57	Infiltrating ductal carcinoma of left breast	2/6	III/III	3.0	30/128	Pos

*Classification of Bloom and Richardson (*31*).
†Values of in vitro quantification of tumor estrogen (ER) and progesterone (PR) receptors in fmol/mg protein. A value of <9 fmol/mg protein is considered negative (Neg).
‡Focal tumor uptake of MIVE.
MIVE = 11β-methoxy-(17α,20E/Z)-[^{123}I]iodovinylestradiol.

tissue radiation dose of 20E/Z isomeric [^{123}I]MIVE in healthy volunteers was calculated, and the specificity of the 20Z isomer for breast tumor ER was evaluated. In healthy volunteers both [^{123}I]MIVE isomers shared a similar tissue distribution pattern. The 20Z isomer, however, cleared at a faster rate from the blood pool, resulting in a higher radioactivity output for the first micturition. Although the 20Z isomer was more prone to deiodination (*18,22*), the more rapid clearance of the 20Z versus the 20E isomer did not correlate with increased excretion of free radioiodine in the urine. Chromatographic analysis instead suggested rapid metabolic conversion of (20Z)-[^{123}I]MIVE to hydrophilic derivatives.

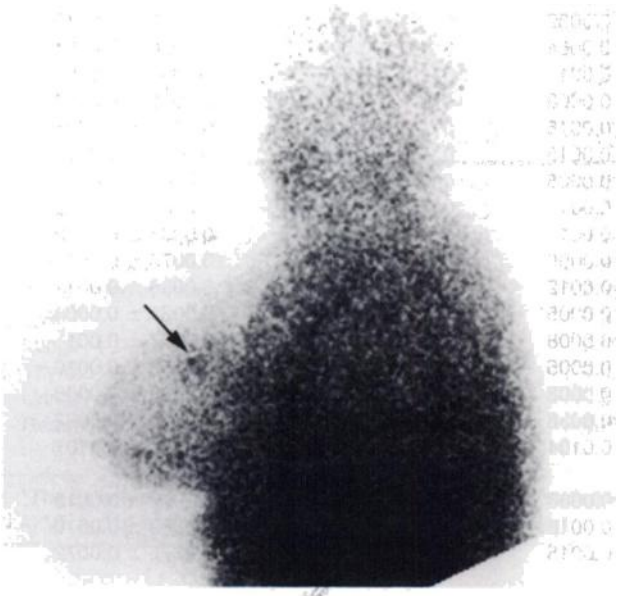

FIGURE 4. Left lateral planar scintigraphic image of 2-cm ER-positive carcinoma (patient 16) 1 h after intravenous administration of (20Z)-[^{123}I]MIVE.

In earlier clinical studies with [^{123}I]MIVE, the radiopharmaceutical was administered as a solution of ethanol and saline (*17,23*). In this study, we used a 20% Intralipid emulsion, which was diluted in saline. Such formulation is appropriate for steroids in view of their lipophilic nature. Uterus uptake studies in immature female rats indicated that formulation of (20Z)-[^{123}I]MIVE in saline and Intralipid did not influence receptor-mediated uterus uptake (unpublished results). We determined that up to 40% of ethanol can be incorporated in Intralipid at room temperature without inducing precipitation of the proteins; in our study the amount of ethanol in the final formulation never exceeded 10%.

Because of a lack of an appropriate phantom, most radiation doses of radiopharmaceuticals reported in the literature pertain to the standard 70-kg man. In view of the specific use of the present radiopharmaceutical, the adult female phantom obviously is a more appropriate model. The radiation dose estimates that we obtained from the adult male phantom resemble those obtained with the adult female model, with the exception of the gastrointestinal track. In the latter case, the dose is underestimated by 20%, resulting in a lower effective dose. Little radioactivity was found in the thyroid because of the administration of saturating doses of potassium iodine. During the 24-h studies, most radioactivity was cleared through the urinary pathway and fecal excretion was relatively slow. An increase in the gastrointestinal tract transit (through proper medication and diet) would

reduce greatly the radiation dose to the abdominal viscera. Our observed residence times and absorbed doses for the isomeric [^{123}I]MIVE were similar to those reported by Rijks et al. (*30*) for the 20Z isomer. The earlier reported values exhibited a larger spread, most likely associated with the less homogeneous population sample compared with this study.

Incubation of (20Z)-[^{125}I]MIVE in vitro, along with the analysis of plasma from healthy volunteers and cancer patients treated with the same radiopharmaceutical, did not show conversion to the 20E isomer. This finding is in contrast with the earlier reported in vivo transformation of the 20Z isomer toward the thermodynamically more stable 20E configuration in the rat (*22*). This discrepancy is puzzling and may relate to the use of different chromatographic systems rather than actual isomeric conversion.

Our tumor uptake data in human patients reveal some differences with the in vitro measurements of ERs. Two patients showed (20Z)-[^{123}I]MIVE uptake in spite of a negative in vitro ER assay. Although this could represent nonspecific uptake of the radiopharmaceutical, it may also reflect true receptor-mediated uptake. In fact, although one of the patients (patient 17) was ER negative, analysis for PR was positive. It has been suggested that PR determination is important because elevated PR levels also are indicative of ER function (*32–34*). Furthermore, ER-negative and PR-positive tumors are rare (<5% of all breast cancers) (*35,36*). Use of the ER-EIA monoclonal kit assay has a few drawbacks, including unreliability in tissue sampling because of heterogeneous ER distribution within the tumor and possible alteration of the ER functionality associated with tissue manipulation (*5–7,37*). Such false-negative in vitro data may explain why some patients respond to tamoxifen treatment in spite of an ER-negative assay (*36,38,39*). In addition, false-positive assays that result from in vitro receptor determination of ERs that have lost their in vivo functionality may lead to a recommendation of hormonal therapy in a situation in which such treatment would be ineffective (*38,39*). Receptor imaging would also provide the opportunity to verify the ER status during the course of therapy and guide appropriate follow-up procedures. Finally, this method also is well adapted for the determination of the ER status of metastases that may differ from that of the primary tumor (*7*).

CONCLUSION

These data show the feasibility of using (20Z)-[^{123}I]MIVE for the in vivo scintigraphic imaging of ER. Tumor uptake was optimal at 1 h after injection and showed a good correlation with in vitro ER analysis. (20Z)-[^{123}I]MIVE is rapidly removed from the blood stream, and possible conversion of its 20E isomer was not observed. Evidently, a larger number of patients need to be tested to validate the usefulness of 20Z-[^{123}I]MIVE in the management of breast cancer patients.

ACKNOWLEDGMENTS

The authors thank MDS Nordion for providing ^{123}I and Dr. Daniel Houde for his help with the excretion model. This work was supported by the Clinical Research Center of the Sherbrooke University Hospital (CUSE), Sherbrooke, Quebec, Canada.

REFERENCES

1. Bertelsen CA, Guiliano AE, Kern DH, Mann BD, Roe DJ, Morton DL. Breast cancer: estrogen and progesterone receptor status as a predictor of *in vitro* chemotherapeutic response. *J Surg Res.* 1984;37:257–263.
2. Clarck GM, Sledge GW Jr, Osborne CK, McGuire WL. Survival from first recurrence: relative importance of prognostic factors in 1,015 breast cancer patients. *J Clin Oncol.* 1987;5:55–61.
3. Rose C, Thorpe SM, Andersen KW, et al. Beneficial effect of adjuvant tamoxifen therapy in primary breast cancer patient with high estrogen receptor values. *Lancet.* 1985;1:16–79.
4. Vollenweider-Zeragui L, Barrelet G, Wong Y, Lemarchand-Béraud T, Gomez F. The predictive value of estrogen and progesterone receptor concentration on the clinical behavior of breast cancer in women. *Cancer.* 1986;57:1171–1180.
5. van Netten JP, Armstrong JB, Carlyle SS, et al. Estrogen receptor distribution in the peripheral intermediate and central regions of breast cancer. *Eur J Cancer Clin Oncol.* 1988;24:1885–1889.
6. Mobbs BG, Fisch EB, Pritchard KI, Oldfield G, Hanna WH. Estrogen and progesterone receptor content of primary and secondary breast carcinoma: influence of time and treatment. *Eur J Cancer Clin Oncol.* 1987;23:819–826.
7. Holdaway IM, Bowditch JV. Variation in receptor status between primary and metastatic breast cancer. *Cancer.* 1983;52:479–485.
8. Schober O, Scheid K, Jackish C, et al. Breast cancer imaging with radioiodinated oestradiol [letter]. *Lancet.* 1990;23:1522.
9. McGuire AH, Dehdashti F, Siegel BA, et al. Positron tomographic assessment of 16α-[^{18}F]fluoro-17β-estradiol uptake in metastatic breast carcinoma. *J Nucl Med.* 1991;32:1526–1531.
10. Dehdashti F, Mortimer JE, Siegel BA, et al. Positron tomographic assessment of estrogen receptors in breast cancer: comparison with FDG-PET and in vitro receptor assays. *J Nucl Med.* 1995;36:1766–1774.
11. Mortimer JE, Dehdashti F, Siegel BA, Katzenellenbogen JA, Fracasso P, Welch MJ. Positron emission tomography with 2-[F-18]fluoro-2-deoxy-D-glucose and 16-alpha-[F-18]fluoro-17-beta-estradiol in breast cancer: correlation with estrogen receptor status and response to systemic therapy. *Clin Cancer Res.* 1996;2:933–939.
12. Preston DF, Spicer JA, Barankzuk RA, et al. Clinical results of breast cancer detection by imageable estradiol (I-123 E_2). *Eur J Nucl Med.* 1990;16:430.
13. Scheidhauer K, Müller S, Smolarz K, Bräutigam P, Briele B. Tumor scintigraphy with 123-I-labeled estradiol for breast cancer receptor scintigraphy [in German]. *Nuklearmedizin.* 1991;30:84–99.
14. Gatley SJ, Shaughnessy WJ, Inhorn L, Lieberman LM. Studies with 17β(16α-[^{125}I]iodo)estradiol, an estrogen receptor-binding radiopharmaceutical, in rats bearing mammary tumors. *J Nucl Med.* 1981;22:459–464.
15. Hanson RN, Seitz DE, Botarro JC. 17α-E-[^{125}I]iodovinyl estradiol: an estrogen-receptor-seeking radiopharmaceutical. *J Nucl Med.* 1982;23:431–436.
16. Jagoda EM, Gibson RE, Goodgold H, et al. [^{125}I]17alpha-iodovinyl 11beta-methoxyestradiol: *in vivo* and *in vitro* properties of a high affinity estrogen-receptor radiopharmaceutical. *J Nucl Med.* 1984;25:472–477.
17. Foulon C, Baulieu JL, Guilloteau D, Bougnoux P, Lansac J, Besnard JC. Estrogen receptor imaging with 17α[^{123}I]iodovinyl-11β-methoxyestradiol (MIVE2). Part II. Preliminary results in patients with breast carcinoma. *Nucl Med Biol Int J Appl Instrum.* 1992;19:263–267.
18. Ali H, Rousseau J, Ghaffari MA, van Lier JE. Synthesis, receptor binding, and tissue distribution of (17α,20E)- and (17α,20Z)-21-[^{125}I]iodo-19-norpregna-1,3,5(10),20-tetraene-3,17-diol. *J Med Chem.* 1988;31:1946–1950.
19. Cummins, CH. Radiolabeled steroidal estrogens in cancer research. *Steroids.* 1993;58:245–259.
20. Ali H, Rousseau J, Ghaffari MA, van Lier JE. Synthesis, receptor binding, and tissue distribution of 7α- and 11β-substituted (17α,20E)- and (17α,20Z)-21-[^{125}I]iodo-19-norpregna-1,3,5(10),20-tetraene-3,17diol. *J Med Chem.* 1991;34:854–860.
21. Rijks LJM, Boer GJ, Endert E, et al. The stereoisomer of the 17α-[^{123}I]iodovinylestradiol and its 11β-methoxy derivative evaluated for their estrogen receptor binding in human MCF-7 cells and rat uterus, and their distribution in immature rats. *Eur J Nucl Med.* 1996;23:295–307.

22. Hughes A, Larson SM, Hanson RN, DeSombre ER. Uptake and interconversion of the Z and E isomers of 17α-iodovinyl-11β-methoxyestradiol in the immature female rat. *Steroids.* 1997;62:244–252.
23. Rijks LJM, Bakker PJM, van Tienhoven G, et al. Imaging of estrogen receptors in primary and metastatic breast cancer patients with iodine-123- labeled Z-MIVE. *J Clin Oncol.* 1997;15:2536–2545.
24. Foulon C, Guilloteau D, Beaulieu JL, et al. Estrogen receptor imaging with 17α(^{123}I)iodovinyl-11β-methoxyestradiol (MIVE2). Part I. Radiotracer preparation and characterization. *Nucl Med Biol Int J Radiat Appl Instrum.* 1992;3:257–261.
25. Hanson RN, Seitz DE, Botarro JC. Radiohalodestannylation: synthesis of E-17α-iodovinyl estradiol. *J Appl Radiat Isot.* 1984;35:810–812.
26. *Pharmakit* [computer program]. Version 3.00 (beta release). London, UK: Johnston A, Woollard R and the University of London; 1990.
27. Graham MM, Peterson LM, Link JM, et al. Fluorine-18-fluoromisonidazole radiation dosimetry in imaging studies. *J Nucl Med.* 1997;38:1631–1636.
28. *MIRDOSE* [computer program]. Version 3.1. Oak Ridge, TN: Oak Ridge Associated Universities; 1995.
29. Stabin MG. MIRDOSE: personal computer software for internal dose assessment in nuclear medicine. *J Nucl Med.*1996;37:538–546.
30. Rijks LJM, Sokole EB, Stabin MG, Debruin K, Janssen AGM, Vanroyen EA. Biodistribution and dosimetry of iodine-123-labelled Z-MIVE: an estrogen receptor radioligand for breast cancer imaging. *Eur J Nucl Med.* 1998;25:40–47.
31. Bloom HJG, Richardson WW. Histological grading and progress in breast cancer: a study of 1409 cases of which 359 have been followed for 15 years. *Br J Cancer.* 1957;11:359–377.
32. Horwitz KB, McGuire WL. Estrogen control of estrogen receptor in human breast cancer. *Cancer.* 1978;253:2223–2228.
33. Horwitz KB, McGuire WL, Pearson OH, Segaloff A. Predicting response to endocrine therapy in human breast cancer: a hypothesis. *Science.* 1975;189:726–727.
34. Ravdin PM, Green S, Dorr TM, et al. Prognostic significance of progesterone receptor levels in estrogen receptor-positive patients with metastatic breast cancer treated with tamoxifen: results of a prospective Southwest Oncology Group study. *J Clin Oncol.* 1992;10:1284–1291.
35. Osborne CK, Yochomowitz MG, Knight WA, McGuire WL. The value of estrogen and progesterone receptors in the treatment of breast cancer. *Cancer.* 1980;46:2884–2888.
36. McGuire WL, Horwitz KB, Pearson OH, Segaloff A. Current status of estrogen and progesterone receptors in breast cancer. *Cancer.* 1977;39:2934–2947.
37. ER-EIA Monoclonal, Technical sheet 66–5364/R7. Abbott Park, IL: Abbott Pharmaceuticals; 1995.
38. Merkel DA, Osborne CK. Use of steroid receptor assays in cancer management. *Rev Endocrinol Rel Cancer.* 1988;30:5–12.
39. McGuire WL, Carbonne PP, Sears ME, Escher GC. In: McGuire WL, Carbonne PP, Volmer EP, eds. *Estrogen Receptors in Human Breast Cancer.* New York, NY: Raven Press; 1975:1–7.